Publications of the Astronomical Society of the Pacific, 136:024203 (13pp), 2024 February https://doi.org/10.1088/1538-3873/ad228e

No X-Rays or Radio from the Nearest Black Holes and Implications for Future Searches

Antonio C. Rodriguez[1], Yvette Cendes[2,3], Kareem El-Badry[1], and Edo Berger[2]
[1] Department of Astronomy, California Institute of Technology, 1200 E. California Blvd, Pasadena, CA 91125, USA; acrodrig@caltech.edu
[2] Center for Astrophysics | Harvard & Smithsonian, 60 Garden Street, Cambridge, MA 02138, USA
[3] Department of Physics, University of Oregon, Eugene, OR 97403, USA

Received 2023 November 9; accepted 2024 January 25; published 2024 February 29

Abstract

Astrometry from the Gaia mission was recently used to discover the two nearest known stellar-mass black holes (BHs), Gaia BH1 and Gaia BH2. These objects are among the first stellar-mass BHs not discovered via X-rays or gravitational waves. Both systems contain $\sim 1\,M_{\odot}$ stars in wide orbits ($a \approx 1.4$ au, 4.96 au) around $\sim 9\,M_{\odot}$ BHs, with both stars (solar-type main sequence star, red giant) well within their Roche lobes in Gaia BH1 and BH2, respectively. However, the BHs are still expected to accrete stellar winds, leading to potentially detectable X-ray or radio emission. Here, we report observations of both systems with the Chandra X-ray Observatory, the Very Large Array (for Gaia BH1) and MeerKAT (for Gaia BH2). We did not detect either system, leading to X-ray upper limits of $L_{\rm X} < 9.4 \times 10^{28}$ and $L_{\rm X} < 4.0 \times 10^{29}\,{\rm erg\,s^{-1}}$ and radio upper limits of $L_r < 1.6 \times 10^{25}$ and $L_r < 1.0 \times 10^{26}\,{\rm erg\,s^{-1}}$ for Gaia BH1 and BH2, respectively. For Gaia BH2, the non-detection implies that the accretion rate near the horizon is much lower than the Bondi rate, consistent with recent models for hot accretion flows. We discuss implications of these non-detections for broader BH searches, concluding that it is unlikely that isolated BHs will be detected via interstellar medium accretion in the near future. We also calculate evolutionary models for the binaries' future evolution using Modules for Experiments in Stellar Astrophysics, and find that Gaia BH1 will be visible as a symbiotic BH X-ray binary for 5–50 Myr. Since no symbiotic BH X-ray binaries are known, this implies either that fewer than $\sim 10^4$ Gaia BH1-like binaries exist in the Milky Way, or that they are common but have evaded detection.

Unified Astronomy Thesaurus concepts: Stellar mass black holes (1611); X-ray binary stars (1811); Accretion (14); Binary stars (154)

1. Introduction

Understanding the full demographics of the stellar-mass black hole (BH) population provides key insights into stellar and galactic evolution. BHs are created by the deaths of some stars with initial masses $M_* \gtrsim 20 M_{\odot}$. Precisely which stars form BHs, and which leave behind neutron stars or no remnant at all, is uncertain (e.g., O'Connor & Ott 2011; Sukhbold et al. 2016; Laplace et al. 2021). The Milky Way has formed $\sim 10^{11}$ stars in its lifetime, and the stellar initial mass function (e.g., Salpeter 1955) dictates that the number of massive stars that have formed, died, and left behind a BH stands at $\sim 10^7$–10^8 (e.g., Sweeney et al. 2022).

Most ($\gtrsim$70%) of these massive stars exist with a binary companion, with triple and higher order systems also being common (Kobulnicky & Fryer 2007; Sana et al. 2012; Moe & Di Stefano 2017). However, the binary fraction of BHs is unknown. Virtually all known or suspected stellar-mass BHs today are in close binaries, in which a stellar companion to a BH is close enough that the BH is accreting significant quantities of gas from it, and the accretion flow produces observable emission across the electromagnetic spectrum. ~20 dynamically confirmed BHs exist in X-ray binaries, ~50 X-ray sources are suspected to contain a BH based on their X-ray properties (e.g., McClintock & Remillard 2006; Corral-Santana et al. 2016), and a few X-ray quiet binaries have been reported in which a BH is suspected on dynamical grounds (e.g., Giesers et al. 2018, 2019; Mahy et al. 2022; Shenar et al. 2022). Just one isolated BH candidate has been discovered via microlensing (Lam et al. 2022; Mróz et al. 2022; Sahu et al. 2022).

In X-ray bright systems, a BH accretes material from a close companion through stable Roche lobe overflow (RLOF) or stellar winds (e.g., McClintock & Remillard 2006). These systems are called X-ray binaries (XRBs), and are often placed into three distinct spectral/temporal states: (1) the soft state, where the system is X-ray bright ($L_{\rm X} \sim L_{\rm Edd}$) and dominated by

thermal emission from the accretion disk; (2) the hard state, which can be seen across an intermediate range of luminosities ($L_X \sim 10^{-5.5}$–$10^{-2} L_{Edd}$) and is dominated by power-law emission; and the (3) quiescent state, where the system is very faint ($L_X \lesssim 10^{-5.5} L_{Edd}$) and still dominated by power-law emission (e.g., Remillard & McClintock 2006). All BH XRBs have been discovered in either a persistent high lumionsity state or through transient X-ray nova (outburst) events (e.g., Corral-Santana et al. 2016). X-ray novae are caused by a sudden increase of mass transfer onto the BH, which leads to a dramatic increase in X-ray luminosity from quiescence (e.g., McClintock & Remillard 2006). All-sky X-ray monitors (e.g., MAXI, Swift/Burst Alert Trigger (BAT); Burrows et al. 2005; Matsuoka et al. 2009) have been effective at discovering BH candidates from their X-ray novae across the entire Milky Way for those whose luminosities approach L_{Edd}, and out to a few kpc for those that reach $\sim 10^{-2} L_{Edd}$ (e.g., Corral-Santana et al. 2016). However, the recurrence timescale of these outbursts is under strong debate, and so the total number of BH XRBs in the Galaxy is still quite uncertain (Tanaka & Shibazaki 1996; Maccarone et al. 2022; Mori et al. 2022).

In the last few years, a handful of BHs orbited by luminous stars have been discovered in wider orbits (Giesers et al. 2018; Shenar et al. 2022; El-Badry et al. 2023a, 2023b). These systems are still outnumbered by XRBs, but this is likely a consequence of the very different selection functions of X-ray and optical searches. The few wide systems discovered so far likely represent the tip of a substantial iceberg. In this paper, we focus on Gaia BH1 and BH2, the newest and nearest of these systems. Precision astrometry from the third data release of the Gaia mission (DR3) enabled their discovery, and optical high-resolution spectroscopy confirmed their nature. Gaia BH1 and BH2 are systems with a BH in an orbit with a Sun-like main-sequence star, and a red giant likely in its first ascent of the giant branch, respectively. These systems are unique in currently being the BH binaries with the longest known orbital periods (186, 1277 days), largest binary separations ($a = 1.4$, 4.96 au), and also the closest to Earth (480 pc, 1.16 kpc).

Since both Sun-like stars and red giants have stellar winds (e.g., Parker 1958; Faulkner & Iben 1966), we asked: can we see evidence of wind accretion in Gaia BH1 and BH2? In Section 2, we describe our observations and calculate upper limits for both Gaia BH1 and BH2 based on X-ray data from Chandra/ACIS-S, and radio data from the Very Large Array (VLA) and MeerKAT. In Section 3, we show that under the assumption of Bondi–Hoyle–Littleton (BHL) accretion, we should have seen X-rays and radio from Gaia BH2. We argue that a lack thereof signals that radiatively inefficient accretion is responsible for reduced accretion rates and the subsequent lack of multiwavelength emission. Finally, in Section 4, we explore the prospects of detecting wind accretion onto BHs using rates and efficiencies assuming inefficient accretion flow, either through a red giant companion or from the interstellar medium (ISM). We show that surveys such as SRG/eROSITA and pointed observations from Chandra are at best sensitive to (1) BHs accreting from $\sim 100 R_\odot$ red giants and (2) BHs accreting from high density ($n \gtrsim 10^3$ cm^{-3}) H_2 regions while traveling at very low ($\lesssim 5$ km s^{-1}) speeds. Finally, we present Modules for Experiments in Stellar Astrophysics (MESA) models for the future evolution of both systems and their expected X-ray luminosities. Based on these models and the lack of detections of symbiotic BH XRBs from all-sky surveys, we conclude that at most $\sim 10^4$ systems similar to either Gaia BH1 or BH2 exist in the Milky Way, unless a substantial population of symbiotic BH XRBs have evaded detection so far.

2. Data

2.1. X-Ray

We observed Gaia BH1 with the Chandra X-ray Observatory (ObsID: 27524; PI: Rodriguez) using the Advanced CCD Imaging Spectrometer (ACIS) on 2022 October 31 (UT) for a cumulative time of 21.89 ks (sum of two observations: 12.13 and 9.76 ks). The ACIS-S instrument was used in pointing mode, chosen over ACIS-I for its slight sensitivity advantage. The observations were taken about 9 days before apastron, when the separation between the BH and star was ≈2.01 au.

We observed Gaia BH2 for 20 ks with Chandra on 2023 January 25 (proposal ID 23208881; PI: El-Badry). We also used the ACIS-S configuration, with a spatial resolution of about 1″. The observations were timed to occur near the periastron passage, when the separation between the BH and the star was ≈2.47 au.

The X-ray images of both sources are shown in Figure 1. We first ran the `chandra_repro` tool to reprocess the observations; this creates a new bad pixel file and de-streaks the event file. Since the observation of Gaia BH1 was split into two, we then ran the `reproject_obs` tool to merge both observations with respect to a common World Coordinate System. We then used the `srcflux` tool to estimate the 90% upper limit for detecting a source at the optical positions of Gaia BH1 and BH2. We created a 1″ radius source region (1, 0 counts in Gaia BH1, BH2, respectively) at the optical positions of each source, and a 15″ background region (156, 171 counts in Gaia BH1, BH2, respectively) to the side, away from any obvious sources. This tool uses Poisson statistics, as pertinent to X-ray observations and described in Kashyap et al. (2010), to calculate upper flux limits. This is unique from estimating the (false negative) case in which a source is not detected due to confusion with the background rate; in both observations the background rate is very low and the upper limit obtained this way with the `aplimits` tool is similar to our reported value. We detect no significant flux at the location of either system and obtain a 90% upper limit of (1.94×10^{-4}, 1.45×10^{-4} cts s^{-1}), for Gaia BH1 and BH2 respectively. We note that these values are consistent with the 90% upper limits obtained when detecting $n = 1$, 0

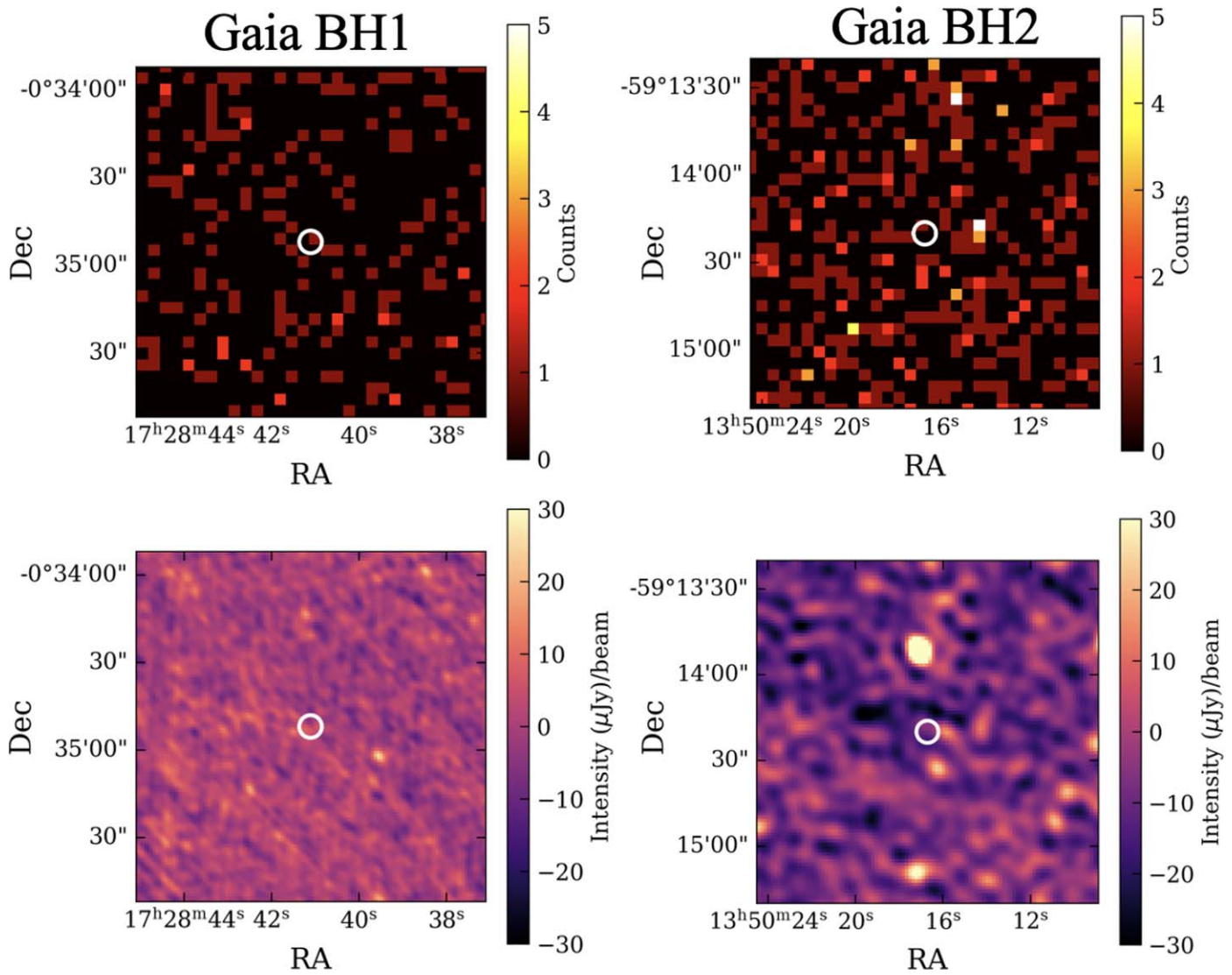

Figure 1. Images of Gaia BH1 (left panels) and Gaia BH2 (right panels) in the X-ray (upper panels) and the radio (lower panels). Both sources were observed for ≈20 ks with Chandra/ACIS-S, corresponding to a flux limit of $\sim 4 \times 10^{-15}$ erg s^{-1} cm^{-2}. Gaia BH1 was observed with the VLA for ≈4 hr, and Gaia BH2 was observed with MeerKAT for ≈4 hr. No significant source of flux is detected at the position of Gaia BH1 or BH2 in either X-rays or radio.

photons in the source region in a 20 ks exposure, as tabulated by Gehrels (1986).

In order to convert to unabsorbed flux, we assume a power-law spectrum with index of 2, and calculate the Galactic hydrogen column density using the relation from Güver & Özel (2009) and the value of A_V from Green et al. (2019), Lallement et al. (2022)—$A_V = 0.93 \pm 0.1$, 0.62 ± 0.1 for BH1, BH2, respectively. Using the PIMMS tool, we calculate an unabsorbed X-ray flux of $F_X = 3.58 \times 10^{-15}$ erg s^{-1} cm^{-2} (BH1) and $F_X = 2.58 \times 10^{-15}$ erg s^{-1} cm^{-2} (BH2) in the 0.5–7 keV energy range. With the Gaia distances, we can calculate the upper limit of the luminosity, which we present in Table 1.

2.2. Radio

We observed Gaia BH1 for 4 hr with the VLA in *C* band (4–8 GHz) in the "C" configuration on 2022 November 27–28 (DDT 22B-294; PI: Cendes). At this time, Gaia BH1 was 17 days past apastron, and the separation between the BH and star was ≈1.98 au. We used the flux calibrator 3C 286 and the gain calibrator J1743-0350. Data was calibrated using the Common Astronomy Software Applications software. We measured the flux density using the imtool package within pwkit (Williams et al. 2017) at the location of Gaia BH1. The rms at the source's position is 3.4 μJy, and we present flux and luminosity 3σ upper limits in Table 1.

Table 1
X-Ray and Radio Upper Limits on Flux and Luminosity (90% Upper Limits in X-Ray, 3σ in Radio)

Object	Facility	Energy Range	BH–Star Separation	Flux Limit	Luminosity Limit
Gaia BH1	Chandra/ACIS-S	0.5–7 keV	2.01 au	$<3.6 \times 10^{-15}$ erg s^{-1} cm^{-2}	$<9.4 \times 10^{28}$ erg s^{-1}
Gaia BH1	VLA/C band	4–8 GHz	1.98 au	<10.2 μJy	$<1.6 \times 10^{25}$ erg s^{-1}
Gaia BH2	Chandra/ACIS-S	0.5–7 keV	2.47 au	$<2.6 \times 10^{-15}$ erg s^{-1} cm^{-2}	$<4.0 \times 10^{29}$ erg s^{-1}
Gaia BH2	MeerKAT/L band	0.86–1.71 GHz	2.54 au	<51 μJy	$<1.0 \times 10^{26}$ erg s^{-1}

We observed Gaia BH2 for 4 hr with the MeerKAT radio telescope in L band (0.86–1.71 GHz) on 2023 January 13 (DDT-20230103-YC01; PI: Cendes), when the separation between the BH and the star was ≈2.54 au. We used the flux calibrator J1939-6342 and the gain calibrator J1424-4913, and used the calibrated images obtained via the SARAO Science Data Processor (SDP)4 for our analysis. We measured the flux density using the imtool package within pwkit (Williams et al. 2017) at the location of Gaia BH2. The rms at the source's position is 17 μJy, and we present X-ray flux, radio flux density, and luminosity 3σ upper limits in Table 1. Luminosities are calculated using $L = 4\pi d^2 F$, where $F = \nu S_\nu$ and ν is the central frequency of the radio band.

We show cutouts of all X-ray and radio images in Figure 1. No significant source of flux is detected at the position of Gaia BH1 or BH2 in either X-rays or radio.

3. Theoretical Predictions

3.1. X-Ray Estimates

We first calculate the X-ray luminosity expected if the BHs accrete their companion stars' winds at the BHL rate:

$$\dot{M}_{\rm BHL} = \frac{4\pi G^2 M_{\rm BH}^2 \rho}{(v^2 + c_s^2)^{3/2}} = \frac{G^2 M_{\rm BH}^2 \dot{M}_{\rm wind}}{v_{\rm wind}^4 d_{\rm sep}^2} \quad (1)$$

where $d_{\rm sep}$ is the separation between the star and BH (which varies as a function of position along the orbit in an elliptical orbit), $M_{\rm BH}$ is the mass of the BH, ρ is the density of accreted material, $\dot{M}_{\rm wind}$ is the mass loss rate of the donor, c_s is the sound speed, v is the relative velocity between the BH and the accreted material, and $v_{\rm wind}$ is the wind speed. We note that the second equality assumes the relative velocity between the BH and accreted material (i.e., the wind speed) greatly exceeds the sound speed. We assume that a fraction η of the accreted rest mass is converted to X-rays, leading to an observable X-ray flux:

$$F_{\rm X,BHL} = \frac{\eta \dot{M}_{\rm BHL} c^2}{4\pi d^2} = \frac{G^2 c^2 M_{\rm BH}^2}{4\pi d^2 d_{\rm sep}^2} \frac{\eta \dot{M}_{\rm wind}}{v_{\rm wind}^4} \quad (2)$$

where d is the distance to the system from Earth. We are left with an X-ray flux that depends on three unknown physical quantities: $\dot{M}_{\rm wind}$, the mass loss rate of the donor star due to winds, $v_{\rm wind}$, the wind speed, and η, the radiative efficiency of accretion. It is important to note that η may vary with accretion rate, or with other properties of the accretion flow.

The donor star in Gaia BH1 is a main-sequence Sun-like star (G dwarf), while the donor in Gaia BH2 is a lower red giant ($R \sim 8\,R_\odot$). Since the donor in Gaia BH1 closely resembles the Sun, and abundance measurements point to it being $\gtrsim$4 Gyr old, we adopt a solar mass loss rate: $\dot{M}_{\rm wind} \approx 2 \times 10^{-14} M_\odot$ yr^{-1} (Wang 1998). Gaia BH2, however, hosts a red giant donor star, which has a mass loss rate strongly dependent on stellar properties. We adopt a simple estimate for its mass loss rate from Reimers (1975):

$$\dot{M}_{\rm wind} = 4 \times 10^{-13} \beta_R \left(\frac{L_\star}{L_\odot}\right)\left(\frac{R_\star}{R_\odot}\right)\left(\frac{M_\star}{M_\odot}\right)^{-1} M_\odot \ {\rm yr}^{-1} \quad (3)$$

where β_R is a scaling parameter for the mass loss rate. We set $\beta_R = 0.1$, following empirical estimates for red giant branch stars (Reimers 1975; Choi et al. 2016). We approximate the wind speed as the escape velocity times a scaling parameter, $\beta_{\rm wind}$:

$$v_{\rm wind} = 600 \beta_{\rm wind} \left(\frac{M_\star}{M_\odot}\right)^{1/2}\left(\frac{R_\star}{R_\odot}\right)^{-1/2} {\rm km\ s^{-1}}. \quad (4)$$

We can then write a scaling relation for Equation (2), assuming fiducial values for Gaia BH1:

$$F_{\rm X,BHL} = 10^{-18}\ {\rm erg\ s^{-1}\ cm^{-2}} \left(\frac{\eta}{10^{-4}}\right)\left(\frac{M_{\rm BH}}{10\,M_\odot}\right)^2 \times \left(\frac{d_{\rm sep}}{2.03\ {\rm au}}\right)^{-2}\left(\frac{d}{480\ {\rm pc}}\right)^{-2} \times \left(\frac{\dot{M}_{\rm wind}}{2 \times 10^{-14} M_\odot\ {\rm yr^{-1}}}\right) \times \left(\frac{v_{\rm wind}}{600\ {\rm km\ s^{-1}}}\right)^{-4} \quad (5)$$

and Equations (3) and (4) can be substituted in for Gaia BH2. We plot the expected X-ray flux from Gaia BH1 and BH2 for a range of possible wind speeds and accretion efficiencies in Figure 2.

Figure 2 shows that a 20 ks Chandra observation should only be able to detect Gaia BH1 if accretion were radiatively efficient ($\eta \gtrsim 0.1$, depending on wind speed). Due to the high wind speed and low mass loss rate, Gaia BH1 is nowhere near its Eddington luminosity and should not experience radiatively

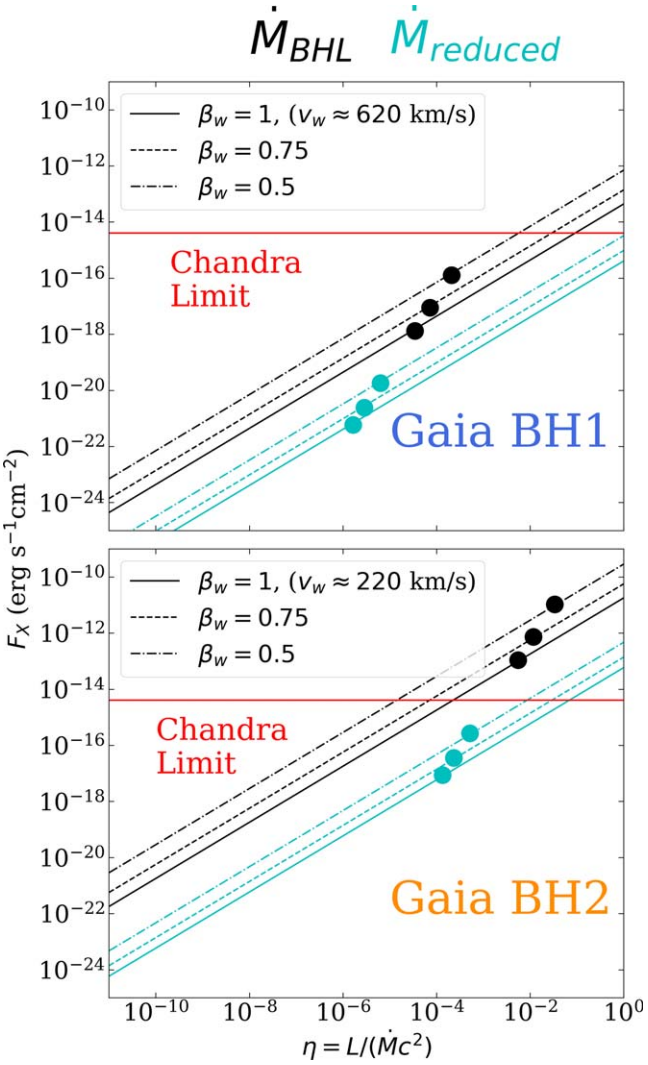

Figure 2. For all plausible wind speeds under the assumption of BHL accretion (black lines), Chandra should have detected X-rays from Gaia BH1 if the accretion flow were radiatively efficient ($\eta \gtrsim 0.1$; top panel) and from Gaia BH2 if the accretion flow were radiatively *in*efficient down to $\eta \gtrsim 10^{-4}$ (bottom panel). Black dots show expected efficiencies from models of hot accretion flows, but assuming the BHL accretion rate. Neither system is detected in X-rays, due to a combination of reduced accretion rates compared to the BHL assumption (cyan lines), and ensuing lower radiative efficiencies (cyan dots).

efficient accretion. Indeed, no X-rays are detected from Gaia BH1, which supports this prediction.

Because of the much stronger wind expected for Gaia BH2, it should have approximately 100 times the X-ray flux of Gaia BH1 under the assumption of BHL accretion. This is despite Gaia BH2 being over twice as distant as Gaia BH1. Remarkably, Gaia BH2 would be within the detection threshold of a 20 ks Chandra ACIS observation for any values of $\eta_X \gtrsim 10^{-4}$. This also applies for any wind slower than the escape velocity ($\beta_w < 1$), which is to be expected as the wind slows down farther from the star. Figure 2 shows that a 20 ks Chandra observation should be able to detect Gaia BH2 down to the case of radiatively *in*efficient flow: $\eta \gtrsim 3 \times 10^{-3}$ if the wind speed is the escape velocity and $\eta \gtrsim 10^{-4}$ if the wind slows by the time it escapes from the star and reaches the BH. However, no X-rays were detected from Gaia BH2, indicating that the radiative efficiency is $\eta < 3 \times 10^{-3}$. In Figure 2, we show the expected accretion efficiencies (black dots; assuming BHL accretion rates) using the hot accretion flow models of Xie & Yuan (2012), which we will further describe in the following subsection. While these models may not be appropriate for obtaining estimates of accretion efficiency under BHL accretion, the X-ray non-detection of Gaia BH2 shows that reduced *accretion rates*, not just low efficiency at BHL rates, must be invoked to explain this non-detection.

3.2. Evidence of Reduced Accretion Rate and Inefficient Accretion in Gaia BH2

The nondetection of X-rays in Gaia BH2 can be explained by going back to Equation (5). The two most uncertain parameters in that equation are the accretion rate at the BH event horizon, $\dot{M}$, as well as the accretion efficiency, η. Indeed, the former causes a change in the latter (e.g., Xie & Yuan 2012). We suggest that in Gaia BH2, the X-ray non-detection is due to $\dot{M}$ being lower than the BHL assumption, which also leads to a lower radiative efficiency. This has been seen in other highly sub-Eddington accreting BHs such as the Milky Way's supermassive BH, Sgr A* (e.g., Yuan et al. 2003), as well as two stellar mass BHs in LMXBs which have been famously well-studied in quiescence: A0620-00 and V404 Cyg (e.g., Narayan et al. 1996, 1997).

In all of these systems, a similar reduction in X-rays is seen, and explained by either advection dominated accretion flows, or luminous hot accretion flows, both of which fall under the class of hot accretion flows (e.g., Xie & Yuan 2012; Yuan et al. 2012). Most of the energy dissipated by viscosity is stored as entropy rather than being radiated away (e.g., through X-rays).

Models of hot accretion flows lead to a reduced accretion rate near the BH event horizon, with $\dot{M} \propto r^s$, where $0 < s < 1$. A general description is presented in Yuan et al. (2012), where it is found that $s \approx 0.5$ and that the accretion rate within $10R_s$ (R_s being the Schwarzschild radius) is approximate constant. This leads to the following reduction to BHL accretion:

$$\dot{M}_{\rm horizon} = \dot{M}_{\rm BHL}\left(\frac{10R_s}{R_{\rm acc}}\right)^{0.5} = \frac{\sqrt{20}\,v_{\rm wind}}{c}\dot{M}_{\rm BHL} \qquad (6)$$

where $R_{\rm acc} = GM_{\rm BH}/v_w^2$ is the characteristic radius of accretion. In the case of Gaia BH1, this leads to $\dot{M} \approx 0.009\dot{M}_{\rm BHL}$ in Gaia BH1 and $\dot{M} \approx 0.003\dot{M}_{\rm BHL}$ in Gaia BH2.

With a more realistic accretion rate in hand, there is one more correction that we can make, which is to use values of radiative

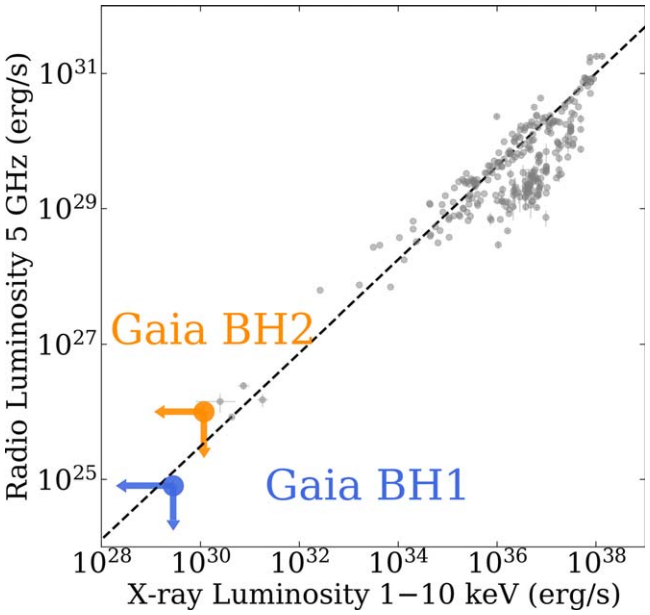

Figure 3. Gaia BH1 and BH2 could lie on the BH "Fundamental Plane." In gray are all measurements of hard state galactic BHs. The dotted line shows the BH fundamental plane from Plotkin et al. (2012) for 10 $M_\odot$ BHs.

efficiency, η, computed for hot accretion flows by Xie & Yuan (2012). Both accretion rates are highly sub-Eddington: $L_{\rm Edd} = 0.1\dot{M}_{\rm Edd}c^2 \Longrightarrow \dot{M}_{\rm Edd} \approx 2 \times 10^{-7} M_\odot\ {\rm yr}^{-1}$ for both Gaia BH1 and BH2. Gaia BH1 has a predicted accretion rate at the horizon of $\dot{M} \approx 0.009\dot{M}_{\rm BHL} \approx 5 \times 10^{-12}\dot{M}_{\rm Edd}$ and Gaia BH2 has an accretion rate of $\dot{M} \approx 0.003\dot{M}_{\rm BHL} \approx 5 \times 10^{-9}\dot{M}_{\rm Edd}$. The same fitting equation is appropriate for both systems:

$$\eta \approx 1.58\left(100 \times \frac{\dot{M}}{\dot{M}_{\rm Edd}}\right)^{0.65} \quad (7)$$

which leads to $\eta \approx 10^{-6}$–10^{-5} for Gaia BH1 and $\eta \approx 10^{-4}$–10^{-3} for Gaia BH2 (cyan dots in Figure 2).

Finally, by substituting both (1) the reduced accretion rate and (2) the corresponding radiative efficiency into Equation (5), we obtain X-ray flux estimates of Gaia BH1 and BH2 to be 10^{-22}–$10^{-20}\,{\rm erg\,s^{-1}\,cm^{-2}}$ and 10^{-18}–$10^{-16}\,{\rm erg\,s^{-1}\,cm^{-2}}$, respectively, which we show with cyan curves in Figure 2. This places both systems well under the Chandra detection limit, but may be within the limits of future missions.

3.3. Radio Estimates

The empirical Fundamental Plane of BH activity relates X-ray luminosity, radio luminosity and BH mass of Galactic BHs and their supermassive analogues (Plotkin et al. 2012). By placing BHs on the Fundamental Plane, the physical process behind BH X-ray and radio emission can be understood. We reproduce the most current compilation of hard state Galactic BHs with measured X-ray and radio luminosities (Bahramian et al. 2018; Plotkin et al. 2021) with upper limits of Gaia BH1 and BH2 overplotted in Figure 3. There is a minor correction to convert to the same X-ray energy ranges and radio frequency ranges, which we omit since it is of order unity. We plot a dotted line to represent the Fundamental Plane for 10$M_\odot$ BHs, and note that BH masses have been estimated (with a $\sim$1 dex uncertainty) from X-ray and radio luminosities (e.g., Gültekin et al. 2019).

If we assume that the Fundamental Plane holds for our systems, and our assumptions of reduced accretion rate and inefficient accretion flow, we can calculate the expected radio luminosities/fluxes: $\sim 10^{21}\,{\rm erg\,s^{-1}}/\sim$1 nJy at 5 GHz (BH1) and $\sim 10^{23}\,{\rm erg\,s^{-1}}/\sim$10 nJy at 5 GHz (BH2). These radio flux densities are well under the projections for future facilities such as the Next Generation VLA (ngVLA; Murphy et al. 2018). Other works, however, have focused on the radio regime and outlined the prospects of detecting isolated BHs in radio surveys, which strongly depends on the Fundamental Plane ($L_{\rm X}$–L_r–mass relation) for radio luminosity calculations (e.g., Maccarone 2005; Fender et al. 2013). We therefore proceed with a discussion of finding BHs solely in the X-ray.

4. Implications for X-Ray Searches of BHs

If no X-ray or radio signatures of accretion are seen from targeted observations of the two nearest known BHs, then what can we expect from blind searches? In the following subsections, we explore the prospects of detecting in the X-ray, (1) wind-accreting BHs in binary systems similar to Gaia BH2, and (2) isolated BHs accreting from the ISM. While other studies have done similar computations in the past (e.g., Agol & Kamionkowski 2002), we incorporate the modern models of inefficient accretion flow and reduced accretion rates (compared to BHL) which we used to explain the X-ray non-detection of Gaia BH2.

4.1. Wind Accreting BHs in Binaries

Are wind-accreting binaries like Gaia BH2 detectable by current X-ray missions? From Equations (3), (4) and (5), it is clear that systems with (1) a closer separation or (2) a star with a larger radius will lead to a larger X-ray luminosity.

Since Sun-like stars that ascend the red giant branch keep their temperatures roughly constant but swell up to $\sim 100R_\odot$, one could expect systems like this to be strong X-ray emitters. In Figure 4, we show the prospects of finding systems similar to Gaia BH2 from X-ray searches alone. We use Equations (4) and (3), to calculate wind speeds and mass loss rates, and Equations (6) and (7) to calculate efficiency and reduced accretion rate corrections from hot accretion flows, as we did for Gaia BH2.

In the top panel of Figure 4, we plot the X-ray flux as a function of orbital period for a system with all other parameters the same as Gaia BH2 ($M_{\rm BH} = 9M_\odot$, $R_* = 8R_\odot$, $e = 0.5$, $d = 1.16$ kpc), and observed at periastron.

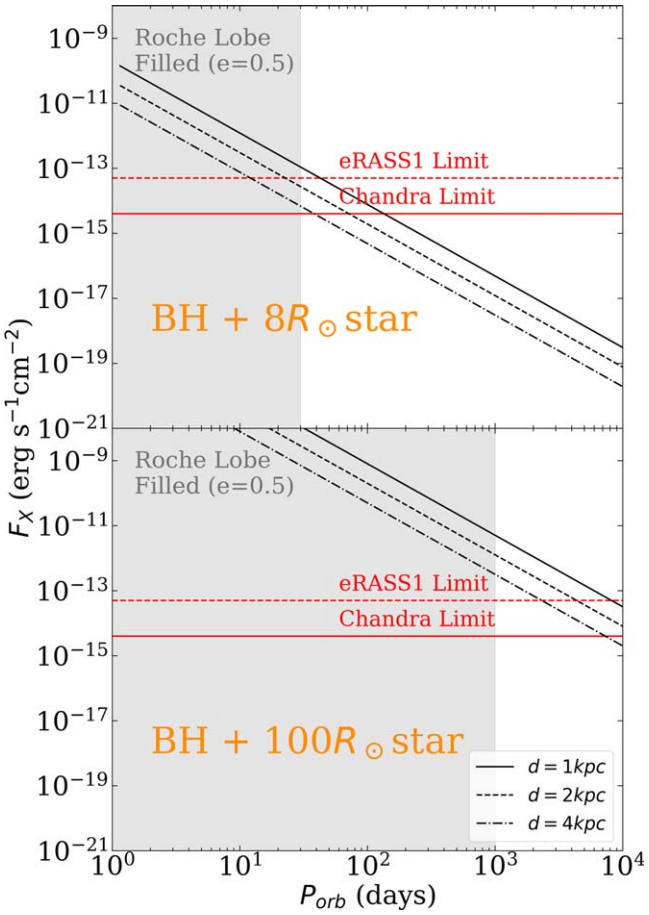

Figure 4. Top: even if Gaia BH2-like system had a shorter orbital period, it would not be detectable in X-rays before filling its Roche lobe (gray shaded area). Bottom: a BH in a binary with a tip of the red giant branch star ($R_* \sim 100R_\odot$) can be bright enough in X-rays for the system to be detectable before the star fills its Roche lobe ($P_{\rm orb} \approx 10^3$–10^4 days).

Even if a Gaia BH2-like system (i.e., a BH and an $8R_\odot$ giant) were in a shorter period orbit, it would not be detectable before filling its Roche lobe ($P_{\rm orb} \approx 30$ days). At this point, an accretion disk could form, which could lead to higher radiative efficiency and/or outbursts that could lead to the system being more easily detectable in X-rays. Such calculations are the subject of Section 5, where we explore the prospects of detecting systems similar to Gaia BH1 and BH2 when filling their Roche lobes.

In the bottom panel of Figure 4, we plot the X-ray flux as a function of orbital period for a system that could resemble what Gaia BH2 will look like in 100 Myr, when the red giant reaches the tip of the red giant branch ($M_{\rm BH} = 9M_\odot$, $R_* = 100R_\odot$, $e = 0.5$). We plot the X-ray flux for a system at 1, 2, and 4 kpc. Such a system would fill its Roche lobe at $P_{\rm orb} \sim 10^3$ days, but systems in the range of $P_{\rm orb} \sim 10^3$–10^4 days are detectable by Chandra out to a few kpc, depending on the exact orbital period. In Figure 4 and following figures, we adopt a Chandra flux limit of 4×10^{-15} erg s^{-1} cm^{-2}, approximately corresponding to the 90% flux limits presented in this paper in a 20 ks exposure, We also show a flux limit of 5×10^{-14} erg s^{-1} cm^{-2} from a single all-sky scan of the SRG/eROSITA mission—eRASS1 is the name of the first all sky scan, though co-adds of multiple scans go deeper (Predehl et al. 2021; Sunyaev et al. 2021). This means that wind-accreting BHs in binaries could be detectable in X-rays before the donor stars fill their Roche lobes. However, this is only the case for appreciable eccentricities $e \gtrsim 0.5$. Circular orbits (as might be more likely for $R_* \sim 100R_\odot$ donors due to tidal circularization), would lead to a 75% decease in flux, pushing the limits of Chandra.

4.2. BHs Accreting from the ISM

We compute the observed X-ray flux from a BH accreting from the ISM. This could be either an isolated BH or a BH in a binary or higher-order system, as long as it is accreting from the ISM. Previous works assumed a BHL accretion rate (e.g., Agol & Kamionkowski 2002), whereas we use the corrected accretion rates and efficiencies from Yuan et al. (2012) and Xie & Yuan (2012), respectively, as supported by the non-detection of Gaia BH2.

The ISM is made up of at least 5 phases, ordered from most to least dense: gravitationally bound giant molecular clouds made up of molecular hydrogen, diffuse H_2 regions, the cold neutral medium (CNM), warm neutral medium, and warm ionized medium (e.g., Draine 2011). All phases of the ISM have been found to be roughly in pressure equilibrium (i.e., $\rho \times T \sim$ constant; though with a $\sim$1 dex spread). Given that sound speed in a medium is proportional to the square root of temperature: $c_s \propto \sqrt{T}$, from Equation (1), it is already clear that ISM-accreting BHs will be more X-ray bright when passing through the densest regions of the ISM.

We calculate the expected X-ray flux due to a BH accreting from an H_2 region ($\overline{n} \approx 10^3$ cm^{-3}, $T \approx 30$ K) and from the CNM ($\overline{n} \approx 30$ cm^{-3}, $T \approx 100$ K). We take $\rho = m_p n$ and calculate the sound speed as $c_s = \sqrt{k_{\rm B} T / m_p}$. We then use the left hand sides of Equations (1) and (2) and additionally incorporate the hot accretion flow corrections to the accretion rate (Equation (6)) and accretion efficiency (Equation (7)).

We plot the X-ray flux as a function of distance for a BH accreting from the ISM in Figure 5. We present curves for a BH accreting from an H_2 region and the CNM, for BH space velocities of 5 and 50 km s^{-1}. We do not plot curves for higher velocities since the flux levels are reduced dramatically. In other words, isolated BHs with space velocities that exceed 50 km s^{-1} are virtually impossible to detect by current X-ray capabilities. While a few isolated BHs within 100 pc *may* be detectable as faint X-ray sources, it would be difficult to distinguish them from other astrophysical sources at larger distances.

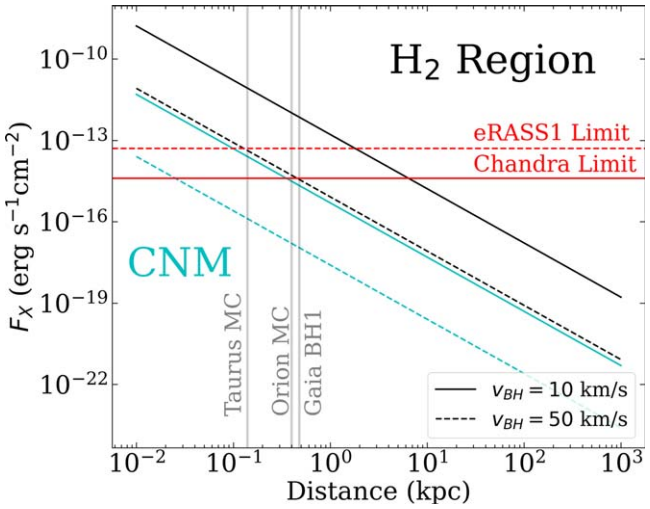

Figure 5. A BH accreting from the ISM in an H_2 region is detectable by current X-ray missions out to a few kpc. However, given that the nearest BH, Gaia BH1, is 480 pc away, it is unlikely to find BHs much nearer than that. With that in mind, the plot above shows that the prospects for detecting BHs accreting from the CNM or any lower density ISM phase are slim to none with current capabilities.

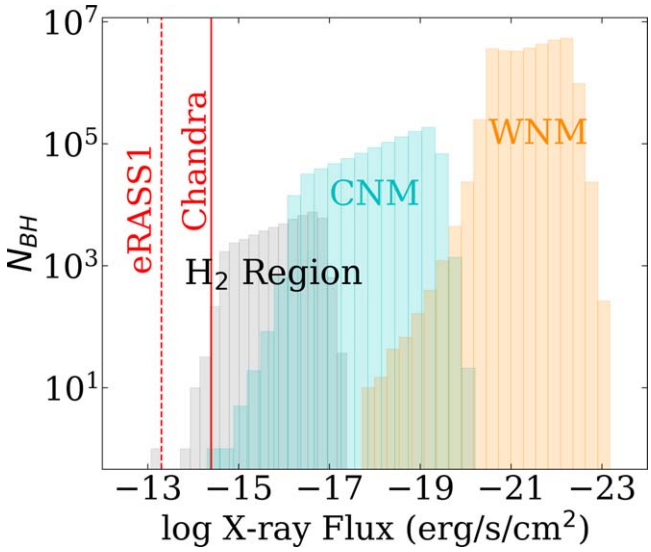

Figure 6. A simple model assuming a distribution of 10^8 stellar-mass BHs passing through the various phases of the ISM in the Milky Way show that the most X-ray bright will be those passing through low density H_2 regions. However, even generous model assumptions suggest that the chances of detecting BHs accreting from the ISM are unlikely after adopting models of hot accretion flows.

Figure 5 shows that a *very* slow-moving BH ($v = 10\,\mathrm{km\,s^{-1}}$) can be detectable if passing through a high-density H_2 region. Such systems are detectable out to $\sim$2 kpc in eRASS1, and $\sim$5 kpc in a 20 ks Chandra pointing. We note that Figure 5 makes the prospects of finding such systems deceptively promising, given the low volume filling factors of H_2 regions. Furthermore, the high column density of hydrogen in H_2 regions is likely to reduce the flux by an appreciable amount, further challenging the prospects of detection.

Given the above calculations for single systems, how many ISM-accreting BHs can be found in the Milky Way? From Equation (1) and Figure 5, it is clear that that $\dot{M}_{\rm BHL} \propto v_{\rm BH}^{-3}$ scaling relation makes the X-ray flux of BHs dramatically decrease given a slight increase in BH space velocity. Currently, the velocity distribution of BHs in binaries is unknown, both due to low-number statistics (only $\sim$20 systems are dynamically confirmed) (Corral-Santana et al. 2016; Atri et al. 2019; Zhao et al. 2023) and due to selection effects in samples of detectable BHs. It is still uncertain if BHs are born with kicks (e.g., Stevenson 2022; Kimball et al. 2023). Furthermore, because there are only a few known BHs in wide binaries and one candidate isolated BH from microlensing, we must assume a velocity distribution.

To investigate an optimistic scenario, we assume the space velocity of ISM-accreting BHs is uniformly distributed between 10 and 50 $\mathrm{km\,s^{-1}}$. We assume that 10^8 BHs are distributed axisymmetrically throughout the Milky Way, exponentially in cylindrical (h, s, ϕ are vertical, radial, and azimuthal coordinates, respectively) h and s coordinates with characterstic scales of 410 pc and 1 kpc, respectively (e.g., van Paradijs & White 1995). We then use the filling factor of each component of the ISM (H_2 region: 0.05%, CNM: 1%, WMN: 30%) to calculate the total number of BHs passing through each region (e.g., Draine 2011). We present the resulting distributions in Figure 6. Based on those results, virtually no ISM-accreting BHs are detectable in eRASS1, but $\sim$10 could be detectable in 20 ks Chandra observations of *all* H_2 regions. However, this number is almost certainly inflated due to the effects of a high column density in H_2 regions and our uncertain assumptions on the BH velocity distribution. It appears improbable to detect X-rays from ISM-accreting BHs passing through the CNM or WMN, given current capabilities.

4.3. Comparison with Previous Work

Previous analyses have been done to estimate the detectability of isolated NSs or BHs accreting from the ISM in the X-ray and/or radio. An early study by Agol & Kamionkowski (2002) projected that all-sky X-ray surveys with the depth of Chandra should detect thousands of isolated BHs. That study, however, operated under the assumption of Bondi accretion, which we have shown is insufficient. Work by Perna et al. (2003) arrived at the same conclusion when calculating the number of isolated NSs detectable by the ROSAT all-sky X-ray survey. As mentioned earlier, works focused on the radio regime strongly rely on the Fundamental Plane ($L_{\rm X}$–L_r–mass relation) for radio luminosity calculations, and initially

predicted that $\sim 10^2$ isolated BHs could be found in the LOFAR survey (Maccarone 2005). However, the more recent work of Fender et al. (2013) found this number to be overestimated and that only systems with high accretion efficiencies could be detectable by the upcoming Square Kilometre Array (SKA) radio survey (we note that SKA will have a depth of $\sim 1\ \mu$Jy (Dewdney et al. 2009), while we estimate that both Gaia BH1 and BH2 have flux densities of 1–10 nJy, as mentioned earlier).

Finally, we note that the recent study by Paduano et al. (2022) undertook an X-ray and radio survey of the globular cluster NGC 3201, where BHs in wide orbits similar to Gaia BH1 and BH2 have been found (NGC 3201 #12560 in a wide, 166 days orbit; NGC 3201 #21859 in a much smaller 2.2 days orbit) (Giesers et al. 2018, 2019). Crucially, we note that NGC 3201 #21859 is reported to be only a *candidate BH system*. They placed both systems on the Fundamental Plane, finding their upper limits to be in agreement. Most importantly, they found upper limits on the accretion efficiency of both systems. NGC 3201 #12560 has an upper limit of $\eta < 0.65$, meaning that our efficiency limits are much deeper. The efficiency limits on NGC 3201 #21859 are much deeper: $\eta < 1.5 \times 10^{-5}$. This means that if that system is indeed a BH system, the efficiency upper limit of Paduano et al. (2022) is consistent with our estimated values for Gaia BH1, which has a main sequence donor star most similar to that in NGC 3201 #21859. In summary, our work shows that due to a combination of reduced accretion rate and radiative efficiency, the chances of detecting ISM- or stellar wind-accreting BHs in blind searches is low, in agreement with recent findings.

5. Future Evolution of Gaia Black Holes and Detection as Symbiotic BH XRBs

We use the expected future evolution of Gaia BH1 and BH2 to understand how common these systems could be in the Milky Way. The discovery paper of Gaia BH1 used the properties of the Gaia DR3 astrometric sample to infer that ~40,000 BH1-like systems should exist (El-Badry et al. 2023b). To constrain the population size, we take a different approach and evolve the Gaia BH1 and BH2 systems using MESA (Paxton et al. 2011, 2013, 2015, 2018). The donor star in Gaia BH1 will become a red giant in a few Gyr, and will ultimately fill its Roche lobe near the tip of the first giant branch. The donor star in Gaia BH2 is already a red giant, and will swell enough to fill its Roche lobe in ~100 Myr at the tip of the asymptotic giant branch. We show their locations in the HR diagram today and during RLOF in Figure 7. We look for the timescales in their evolution when the systems could be visible as symbiotic BH XRBs (i.e., a BH accreting from a red giant filling or nearly filling its Roche lobe).

In the top panels of Figure 8, we show the BH mass loss rates ($\dot{M}$) of the donor star in the Gaia BH1 and BH2 systems for approximately 500 Myr and 10 Myr before RLOF,

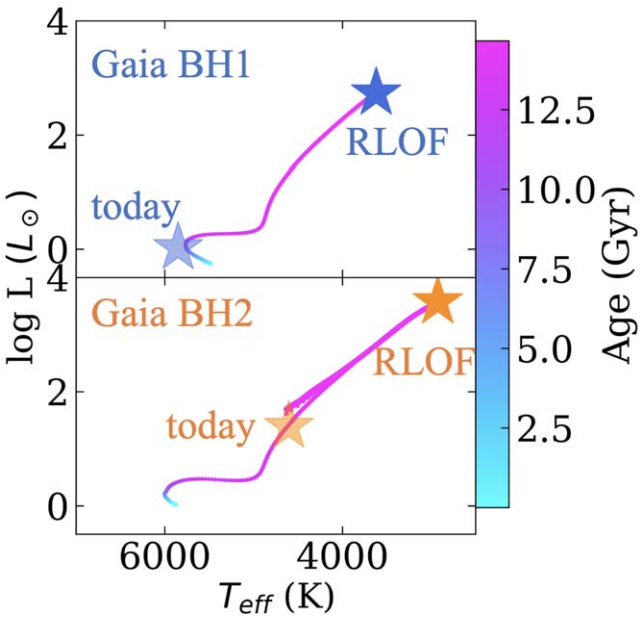

Figure 7. Gaia BH1 will fill its Roche lobe near the tip of its first giant branch in a few Gyr. Gaia BH2 will do so near the tip of the AGB in ~100 Myr. Leading up to this stage, both systems will likely be detectable as symbiotic BH XRBs, yet no such systems have been confirmed to date.

respectively. The bottom panels of Figure 8 zoom in and show where RLOF begins. Before RLOF, wind accretion takes place. For low mass loss rates ($\dot{M} \lesssim 10^{-2}\dot{M}_{\rm Edd,BH}$), the BH accretion rate could be much lower than the donor mass loss rate (as we explain through most of this paper). However, for mass loss rates that approach the Eddington accretion rate of the BH and certainly during RLOF, the two should be nearly equal (e.g., Ritter 1988). It is also worth noting that after RLOF, the donor star will have been stripped of its atmosphere, and the orbit of both systems will expand. The orbital period will increase from 186 days to ≈850 days in Gaia BH1 and from 1277 days to ≈2000 days in Gaia BH2.

In the top panels of Figure 8, we then shade the region where the accretion rate exceeds $10^{-2}\dot{M}_{\rm Edd}$, where we expect the accretion rate is high enough to lead to frequent outbursts, or a persistent state of high luminosity, that could be observed by all-sky X-ray monitors. This accretion rate corresponds to the X-ray lumionsities at which both currently known symbiotic XRBs (albeit with neutron star accretors) have been seen to outburst (e.g., Kuranov & Postnov 2015; Yungelson et al. 2019). We define the timescale during which the Gaia BH systems are seen as symbiotic XRBs as $\tau_{\rm SymXRB}$, which in Gaia BH1 lasts ≈50 Myr and in Gaia BH2 lasts ≈2 Myr. X-ray monitors such as the Swift BAT (Burrows et al. 2005) and MAXI (Matsuoka et al. 2009) have similar sensitivities of ~100 mCrab (10^{-9} erg s^{-1} cm^{-2}) for ~min long exposures. This means that these monitors are sensitive to essentially all

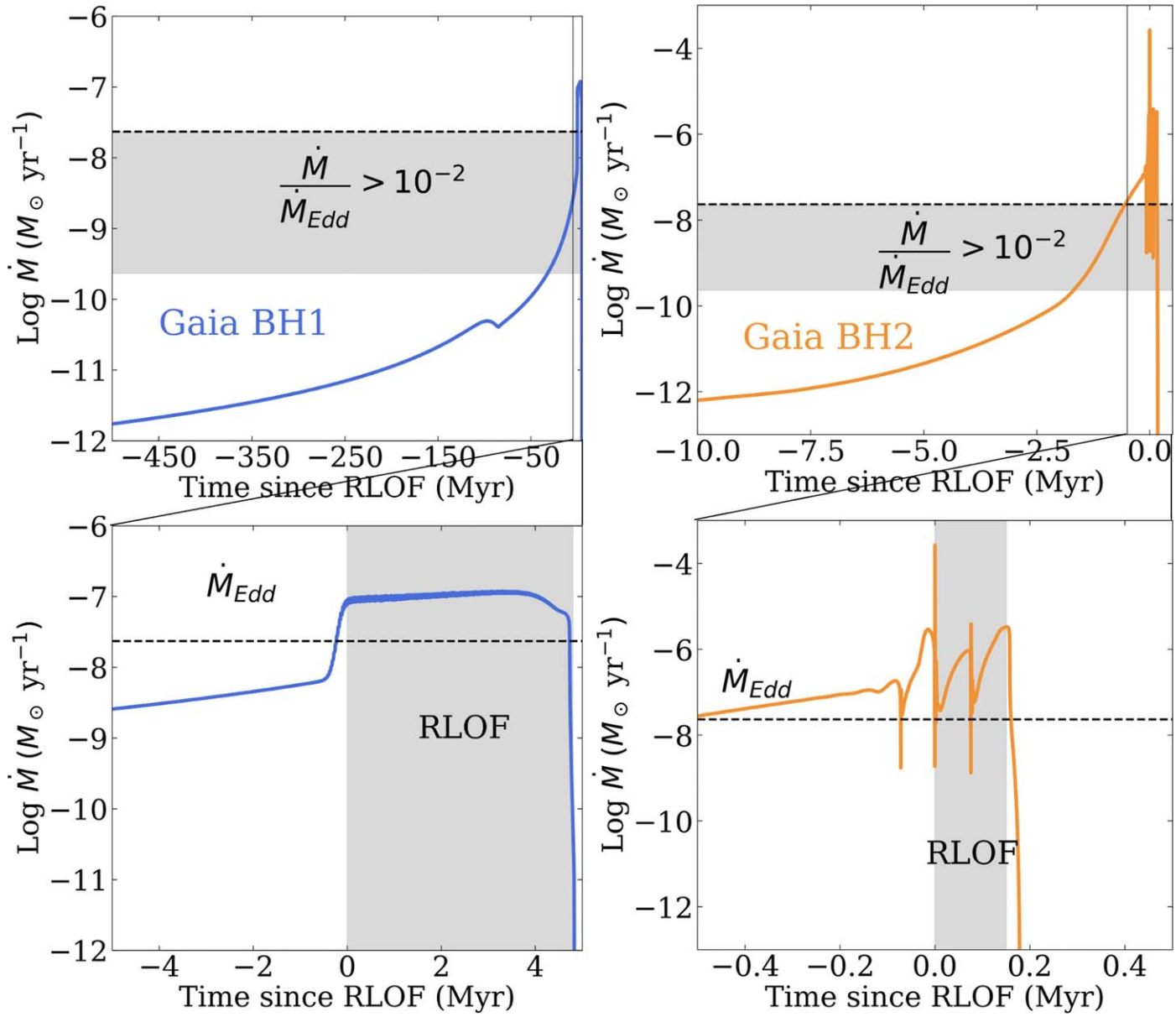

Figure 8. MESA models around the time when the donors fill their Roche lobes show that Gaia BH1 will be visible as a symbiotic BH XRB for ≈50 Myr, while $\dot{M} > 10^{-2}\dot{M}_{\rm Edd}$ (upper left) and for ≈5 Myr, while $\dot{M} \sim \dot{M}_{\rm Edd}$ (lower left). Gaia BH2 will be visible as a symbiotic BH XRB for ≈2 Myr, while $\dot{M} > 10^{-2}\dot{M}_{\rm Edd}$ (upper right) and for ≈0.2 Myr, while $\dot{M} \sim \dot{M}_{\rm Edd}$ (lower right). Because no such systems have been discovered through X-ray outbursts, there should be at most $\sim 10^4$ Gaia BH1-like systems in the Milky Way, unless outburst timescales of such systems have been underestimated.

$L_{\rm X} \sim L_{\rm Edd}$ outbursts in the Galaxy, and sensitive to outbursts $L_{\rm X} \gtrsim 10^{-2} L_{\rm Edd}$ out to a few kpc.

Both Gaia BH1 and BH2 undergo a very short phase where $\dot{M} \gtrsim \dot{M}_{\rm Edd}$ (Gaia BH1 exceeds $\dot{M}_{\rm Edd}$ by a factor of 10, while BH2 reaches factors of 10^2–10^3). Centaurus X-3 is an example of such a system, where extended periods of low X-ray flux have been observed in a pulsar high mass X-ray binary accreting near the Eddington rate. It has been postulated that at the highest accretion rates, matter gathers at the innermost regions of the accretion disk and absorbs the X-rays, leading to extended lows (Schreier et al. 1976). However, this system is still X-ray bright for the majority of the time and detectable by all-sky X-ray monitors. Our models show that Gaia BH1 will be in such a phase for ∼5 Myr, and BH2 for ∼0.2 Myr. In both cases, this phase lasts for ≈10% the duration of the evolution when the systems are in the symbiotic XRB phase (i.e., accretion is sub-Eddington and is due to winds rather than RLOF).

In order to estimate an upper limit on the number of similar systems in the Milky Way, we assume a detection efficiency, $\varepsilon_{\rm detect}$, for all-sky X-ray monitors and take the lifetime of $\sim 1 M_{\odot}$ stars divided by the time during which these systems are visible as symbiotic BH XRBs:

$$N_{\rm BH} \sim \frac{\tau_{\rm stars}}{\varepsilon_{\rm detect}\tau_{\rm SymXRB}}$$
$$N_{\rm BH1} \approx 2 \times 10^2/\varepsilon_{\rm detect}, \quad N_{\rm BH2} \approx 5 \times 10^3/\varepsilon_{\rm detect}. \quad (8)$$

In the case where we use the short-lived phase where the donors are Roche lobe overflowing, the above becomes:

$$N_{\rm BH} \sim \frac{\tau_{\rm stars}}{\varepsilon_{\rm detect}\tau_{\rm RLOF}}$$
$$N_{\rm BH1} \approx 2 \times 10^3/\varepsilon_{\rm detect}, \quad N_{\rm BH2} \approx 5 \times 10^4/\varepsilon_{\rm detect}. \quad (9)$$

During the last $\sim$50 yr, all-sky X-ray surveys have been sensitive to X-ray outbursts from such systems, but no symbiotic BH XRBs have been discovered. From Uhuru (Forman et al. 1978) to MAXI, it is highly unlikely that the brightest X-ray outbursts have been missed. From Equation (9), even if we assume a 10% efficiency ($\varepsilon_{\rm detect} = 0.1$) of all-sky X-ray monitors in detecting such systems, this places Gaia BH1-like systems at $N \lesssim 2 \times 10^3$ and BH2-like systems at $N \lesssim 2 \times 10^4$ in our galaxy. If we assume that systems are only detectable during RLOF, the corresponding limits are $N \lesssim 2 \times 10^4$ and $N \lesssim 2 \times 10^5$.

There is at least one candidate symbiotic XRB proposed to host a BH, IGR J17454-2919 (Paizis et al. 2015). The most accurate Chandra localization of the X-ray source coincides with a red giant (K- to M-type), while the X-ray outburst properties of the system do not securely point to either a NS or BH accretor. Ongoing work is being conducted to determine the nature of this system. A handful of symbiotic XRBs hosting NSs have been detected as X-ray sources even though the donors have not yet overflowed their Roche lobes (e.g., Hinkle et al. 2006, 2019; Masetti et al. 2007; Bozzo et al. 2018; De et al. 2022). That being said, the radiative efficiencies of accreting NSs are likely to be larger than those of BHs (e.g., Garcia et al. 2001), and the accretion rate above which BH symbiotic XRTs are likely to be recognized as such is uncertain.

6. Discussion and Conclusions

We have analyzed X-ray and radio observations of the two nearest known BHs: Gaia BH1 and BH2. For both sources, we only detect upper limits in both the X-ray and radio. Due to the relatively strong, low-velocity winds from the red giant in Gaia BH2, BHL accretion predicts that we should have seen X-rays from the system. We interpret our non-detection as a sign of reduced accretion rates as seen in hot accretion flows, and an ensuing lower radiative efficiency than predicted by BHL accretion. We found that these hot accretion flow corrections lead to X-ray (and radio) fluxes well below the limit of current facilities.

We then used the corrected accretion rates and efficiencies to compute the observed flux from a BH accreting from a $R_* \sim 100 R_{\odot}$ red giant (i.e., what Gaia BH2 will become in 100 Myr). We found that a relatively nearby system ($d \lesssim 4$ kpc) of that type could be detectable in X-rays *before* filling its Roche lobe.

We then extended our calculations to wind-accreting BHs passing through the ISM. We found that the only plausible scenario for detecting such a system would be to have a very slowly moving ($v \lesssim 10\,{\rm km\,s^{-1}}$) BH passing through a dense ($n \gtrsim 10^3\,{\rm cm^{-3}}$) H_2 region. Current technologies rule out the possibility of detecting an ISM-accreting BH passing through the CNM or any lower density phase of the ISM, even with generous assumptions about BH velocity and the population distribution.

Finally, we produced MESA models of the future evolution of Gaia BH1 and BH2. We predict that the accretion rate in Gaia BH1 will be high enough ($\dot{M} \sim 10^{-2}\dot{M}_{\rm Edd}$) for the system to be visible as a symbiotic BH XRB for $\approx$50 Myr. The same will be true for Gaia BH2, but only for $\approx$2 Myr. Although the symbiotic BH XRB phase is a relatively short-lived phase in the evolution of these systems, the effective search volume for X-ray bright systems is large. Because all-sky X-ray monitors have been sensitive to X-ray outbursts in a large part of the Galaxy for the last $\approx$50 yr, the lack of detected symbiotic BH XRBs would seem to imply an upper limit on the number of Gaia BH1-like systems at $N \lesssim 10^3$ (10^4 assuming 10% detection efficiency), assuming BH + giant systems could be detected anywhere in the galaxy when the BH accretes at a rate $\dot{M} > 10^{-2}\dot{M}_{\rm Edd}$.

This limit is somewhat puzzling. El-Badry et al. (2023b) estimated that the effective search volume for Gaia BH1-like systems in Gaia DR3 was only $\sim 3 \times 10^6$ stars, which would seem to suggest that $>10^4$ similar systems should exist in the Milky Way. There are several possible explanations for these apparently inconsistent limits. One is that symbiotic BH XRBs have already been detected by X-ray surveys but have not been recognized as such. This seems plausible particularly for wind-accretion systems, which may not form disks and undergo outbursts. Such systems would appear as relatively faint X-ray sources coincident with red giants. Many such sources exist in the Galactic plane and have never been studied in detail. These consideration suggest that radial velocity follow-up of giants coincident with X-ray sources may be a promising search strategy for symbiotic BH XRBs.

Another possibility is that the detection efficiency of symbiotic BH XRBs is simply very low. This could be the case if they have unstable disks with very long outburst recurrence timescales, as has indeed been proposed (e.g., Deegan et al. 2009). Furthermore, reddening and crowding in the Galactic plane have been suggested to bias the observed BH

population in low-mass XRBs (e.g., Jonker et al. 2021), which could have an effect on the observability of symbiotic BH XRBs if they were predominantly located there.

The next few years show promise for the discovery of many more BH binaries: SRG/eROSITA in X-rays, Gaia through optical astrometry, and the Rubin Legacy Survey of Space and Time (LSST) through optical photometry. X-ray and radio detections (and non-detections) of future systems will provide new clues regarding the nature of accretion around BHs in a wide range of astrophysical scenarios.

Acknowledgments

We thank Tim Cunningham for a useful discussion on optimal reduction of Chandra data. We are grateful to the Chandra, VLA, and MeerKAT directorial offices and support staff for prompt assistance with DDT observations. The MeerKAT telescope is operated by the South African Radio Astronomy Observatory, which is a facility of the National Research Foundation, an agency of the Department of Science and Innovation. We thank the referee for useful input that led to an improved final manuscript.

A.C.R. acknowledges support from an NSF Graduate Research Fellowship. A.C.R. thanks the LSSTC Data Science Fellowship Program, which is funded by LSSTC, NSF Cybertraining Grant #1829740, the Brinson Foundation, and the Moore Foundation; his participation in the program has benefited this work. K.E. was supported in part by NSF grant AST-2307232.

ORCID iDs

Antonio C. Rodriguez https://orcid.org/0000-0003-4189-9668

References

Agol, E., & Kamionkowski, M. 2002, MNRAS, 334, 553
Atri, P., Miller-Jones, J. C. A., Bahramian, A., et al. 2019, MNRAS, 489, 3116
Bahramian, A., Miller-Jones, J., Strader, J., et al. 2018, Radio/X-ray Correlation Database for X-ray Binaries, v0.1, Zenodo, doi:10.5281/zenodo.1252036
Bozzo, E., Bahramian, A., Ferrigno, C., et al. 2018, A&A, 613, A22
Burrows, D. N., Hill, J. E., Nousek, J. A., et al. 2005, SSRv, 120, 165
Choi, J., Dotter, A., Conroy, C., et al. 2016, ApJ, 823, 102
Corral-Santana, J. M., Casares, J., Muñoz-Darias, T., et al. 2016, A&A, 587, A61
De, K., Mereminskiy, I., Soria, R., et al. 2022, ApJ, 935, 36
Deegan, P., Combet, C., & Wynn, G. A. 2009, MNRAS, 400, 1337
Dewdney, P. E., Hall, P. J., Schilizzi, R. T., & Lazio, T. J. L. W. 2009, IEEEP, 97, 1482
Draine, B. T. 2011, Physics of the Interstellar and Intergalactic Medium (Princeton, NJ: Princeton Univ. Press)
El-Badry, K., Rix, H.-W., Cendes, Y., et al. 2023a, MNRAS, 521, 4323
El-Badry, K., Rix, H.-W., Quataert, E., et al. 2023b, MNRAS, 518, 1057
Faulkner, J., & Iben, I. J. 1966, ApJ, 144, 995
Fender, R. P., Maccarone, T. J., & Heywood, I. 2013, MNRAS, 430, 1538
Forman, W., Jones, C., Cominsky, L., et al. 1978, ApJS, 38, 357
Garcia, M. R., McClintock, J. E., Narayan, R., et al. 2001, ApJL, 553, L47
Gehrels, N. 1986, ApJ, 303, 336
Giesers, B., Dreizler, S., Husser, T.-O., et al. 2018, MNRAS, 475, L15
Giesers, B., Kamann, S., Dreizler, S., et al. 2019, A&A, 632, A3
Green, G. M., Schlafly, E., Zucker, C., Speagle, J. S., & Finkbeiner, D. 2019, ApJ, 887, 93
Gültekin, K., King, A. L., Cackett, E. M., et al. 2019, ApJ, 871, 80
Güver, T., & Özel, F. 2009, MNRAS, 400, 2050
Hinkle, K. H., Fekel, F. C., Joyce, R. R., et al. 2006, ApJ, 641, 479
Hinkle, K. H., Fekel, F. C., Joyce, R. R., et al. 2019, ApJ, 872, 43
Jonker, P. G., Kaur, K., Stone, N., & Torres, M. A. P. 2021, ApJ, 921, 131
Kashyap, V. L., van Dyk, D. A., Connors, A., et al. 2010, ApJ, 719, 900
Kimball, C., Imperato, S., Kalogera, V., et al. 2023, ApJL, 952, L34
Kobulnicky, H. A., & Fryer, C. L. 2007, ApJ, 670, 747
Kuranov, A. G., & Postnov, K. A. 2015, AstL, 41, 114
Lallement, R., Vergely, J. L., Babusiaux, C., & Cox, N. L. J. 2022, A&A, 661, A147
Lam, C. Y., Lu, J. R., Udalski, A., et al. 2022, ApJL, 933, L23
Laplace, E., Justham, S., Renzo, M., et al. 2021, A&A, 656, A58
Maccarone, T. J. 2005, MNRAS, 360, L30
Maccarone, T. J., Degenaar, N., Tetarenko, B. E., et al. 2022, MNRAS, 512, 2365
Mahy, L., Sana, H., Shenar, T., et al. 2022, A&A, 664, A159
Masetti, N., Landi, R., Pretorius, M. L., et al. 2007, A&A, 470, 331
Matsuoka, M., Kawasaki, K., Ueno, S., et al. 2009, PASJ, 61, 999
McClintock, J. E., & Remillard, R. A. 2006, Compact Stellar X-ray Sources, Vol. 39 (Cambridge, UK: Cambridge Univ. Press), 157, doi:10.48550/arXiv.astro-ph/0306213
Moe, M., & Di Stefano, R. 2017, ApJS, 230, 15
Mori, K., Mandel, S., Hailey, C. J., et al. 2022, arXiv:2204.09812
Mróz, P., Udalski, A., & Gould, A. 2022, ApJL, 937, L24
Murphy, E. J., Bolatto, A., Chatterjee, S., et al. 2018, in ASP Conf. Ser. 517, Science with a Next Generation Very Large Array, ed. E. Murphy (San Francisco, CA: ASP), 3, doi:10.48550/arXiv.1810.07524
Narayan, R., Barret, D., & McClintock, J. E. 1997, ApJ, 482, 448
Narayan, R., McClintock, J. E., & Yi, I. 1996, ApJ, 457, 821
O'Connor, E., & Ott, C. D. 2011, ApJ, 730, 70
Paduano, A., Bahramian, A., Miller-Jones, J. C. A., et al. 2022, MNRAS, 510, 3658
Paizis, A., Nowak, M. A., Rodriguez, J., et al. 2015, ApJ, 808, 34
Parker, E. N. 1958, ApJ, 128, 664
Paxton, B., Bildsten, L., Dotter, A., et al. 2011, ApJS, 192, 3
Paxton, B., Cantiello, M., Arras, P., et al. 2013, ApJS, 208, 4
Paxton, B., Marchant, P., Schwab, J., et al. 2015, ApJS, 220, 15
Paxton, B., Schwab, J., Bauer, E. B., et al. 2018, ApJS, 234, 34
Perna, R., Narayan, R., Rybicki, G., Stella, L., & Treves, A. 2003, ApJ, 594, 936
Plotkin, R. M., Bahramian, A., Miller-Jones, J. C. A., et al. 2021, MNRAS, 503, 3784
Plotkin, R. M., Markoff, S., Kelly, B. C., Körding, E., & Anderson, S. F. 2012, MNRAS, 419, 267
Predehl, P., Andritschke, R., Arefiev, V., et al. 2021, A&A, 647, A1
Reimers, D. 1975, MSRSL, 8, 369
Remillard, R. A., & McClintock, J. E. 2006, ARA&A, 44, 49
Ritter, H. 1988, A&A, 202, 93
Sahu, K. C., Anderson, J., Casertano, S., et al. 2022, ApJ, 933, 83
Salpeter, E. E. 1955, ApJ, 121, 161
Sana, H., de Mink, S. E., de Koter, A., et al. 2012, Sci, 337, 444
Schreier, E. J., Swartz, K., Giacconi, R., Fabbiano, G., & Morin, J. 1976, ApJ, 204, 539
Shenar, T., Sana, H., Mahy, L., et al. 2022, NatAs, 6, 1085
Stevenson, S. 2022, ApJL, 926, L32
Sukhbold, T., Ertl, T., Woosley, S. E., Brown, J. M., & Janka, H. T. 2016, ApJ, 821, 38
Sunyaev, R., Arefiev, V., Babyshkin, V., et al. 2021, A&A, 656, A132
Sweeney, D., Tuthill, P., Sharma, S., & Hirai, R. 2022, MNRAS, 516, 4971
Tanaka, Y., & Shibazaki, N. 1996, ARA&A, 34, 607
van Paradijs, J., & White, N. 1995, ApJL, 447, L33
Wang, Y. M. 1998, in ASP Conf. Ser. 154, Cool Stars, Stellar Systems, and the Sun, ed. R. A. Donahue & J. A. Bookbinder (San Francisco, CA: ASP), 131

Williams, P. K. G., Clavel, M., Newton, E., & Ryzhkov, D., 2017 pwkit: Astronomical Utilities in Python, Astrophysics Source Code Library, ascl:1704.001
Xie, F.-G., & Yuan, F. 2012, MNRAS, 427, 1580
Yuan, F., Quataert, E., & Narayan, R. 2003, ApJ, 598, 301
Yuan, F., Wu, M., & Bu, D. 2012, ApJ, 761, 129
Yungelson, L. R., Kuranov, A. G., & Postnov, K. A. 2019, MNRAS, 485, 851
Zhao, Y., Gandhi, P., Dashwood Brown, C., et al. 2023, MNRAS, 525, 1498